

# Recovering Compressively Sampled Signals Using Partial Support Information

Michael P. Friedlander, Hassan Mansour\*, Rayan Saab, and Özgür Yılmaz

## Abstract

In this paper we study recovery conditions of weighted  $\ell_1$  minimization for signal reconstruction from compressed sensing measurements when partial support information is available. We show that if at least 50% of the (partial) support information is accurate, then weighted  $\ell_1$  minimization is stable and robust under weaker conditions than the analogous conditions for standard  $\ell_1$  minimization. Moreover, weighted  $\ell_1$  minimization provides better bounds on the reconstruction error in terms of the measurement noise and the compressibility of the signal to be recovered. We illustrate our results with extensive numerical experiments on synthetic data and real audio and video signals.

## Index Terms

Compressed sensing, weighted  $\ell_1$  minimization, adaptive recovery.

## I. INTRODUCTION

Compressed sensing (see, e.g., [1]–[3]) is a paradigm for effective acquisition of signals that admit sparse (or approximately sparse) representations in some transform domain. The approach can be used to reliably recover such signals from significantly fewer linear measurements than their ambient dimension. Because a wide range of natural and man-made signals—e.g., audio, natural and seismic images, video, and wideband radio frequency signals—are sparse or approximately sparse in appropriate transform domains, the potential applications of compressed sensing can be immense.

Michael P. Friedlander is with the Department of Computer Science, The University of British Columbia, Vancouver, Canada.

Hassan Mansour is with the Departments of Computer Science and Mathematics, The University of British Columbia, Vancouver, Canada.

Rayan Saab and Özgür Yılmaz are with the Department of Mathematics, The University of British Columbia, Vancouver, Canada.

Let  $\Sigma_k^N := \{x \in \mathbb{R}^N : \|x\|_0 \leq k\}$  be the set of all  $k$ -sparse signals in  $\mathbb{R}^N$ , and let

$$y := Ax + e \quad (1)$$

be a vector of measurements where  $A$  is a known  $n \times N$  measurement matrix, and  $e$  denotes additive noise that satisfies  $\|e\|_2 \leq \epsilon$  for some known  $\epsilon \geq 0$ . Compressed sensing theory states that it is possible to recover  $x \in \Sigma_k^N$  from  $y$  (given  $A$ ) even when  $n \ll N$ , i.e., using very few measurements. For example, when  $e = 0$ , one may recover an estimate  $x^*$  of the signal  $x$  as the solution of the constrained  $\ell_0$  minimization problem

$$\underset{z \in \mathbb{R}^N}{\text{minimize}} \quad \|z\|_0 \quad \text{subject to} \quad Az = y. \quad (2)$$

In fact, using (2), any  $x \in \Sigma_k^N$  can be recovered perfectly using  $n$  measurements when  $n > 2k$  and  $A$  is in general position (see, e.g., [4]). However,  $\ell_0$  minimization is a combinatorial problem and quickly becomes intractable as the dimensions increase. Instead, the convex relaxation

$$\underset{z \in \mathbb{R}^N}{\text{minimize}} \quad \|z\|_1 \quad \text{subject to} \quad \|Az - y\|_2 \leq \epsilon \quad (3)$$

can be used to recover the estimate  $x^*$ . Candés, Romberg and Tao [2] and Donoho [1] show that if  $n \gtrsim k \log(N/k)$ , then  $\ell_1$  minimization (3) can stably and robustly recover  $x$  from “incomplete” and inaccurate measurements  $y = Ax + e$ , where  $A$  is an appropriately chosen  $n \times N$  measurement matrix and  $\|e\|_2 \leq \epsilon$ . Note that compressed sensing is a *non-adaptive* data acquisition technique because the measurement matrix  $A$  does not depend on  $x$ , the signal being measured. Furthermore, the recovery method that we just described is itself non-adaptive because no information on  $x$  is used in (3). Our goal in this paper is to examine a recovery method that is adaptive in the sense that it exploits prior support information on  $x$ ; however, the measurement process remains non-adaptive.

#### A. Compressed sensing with prior support information

The  $\ell_1$  minimization problem (3) does not incorporate any prior information about the support of  $x$ . However, in many applications it may be possible to draw an estimate of the support of the signal or an estimate of its largest coefficients. Other signals such as video and audio exhibit temporal correlation over signal frames that can be exploited to estimate a portion of the support using previously decoded frames.

Consider the example where  $x \in \mathbb{R}^N$  is a compressible signal, i.e., it can be well-approximated by its  $k$  largest-in-magnitude entries, where  $k \ll N$ . If  $x$  represents the discrete cosine transform (DCT) or

wavelet coefficients of an image, then the entries of  $x$  that correspond to the low frequency subbands are most likely to be non-zero and carry most of the energy of the signal [5]. In such cases, it is beneficial to incorporate this information in the recovery algorithm when  $x$  is compressively sampled.

### B. Previous Work

We are especially interested in methods that incorporate prior support information by replacing the  $\ell_1$  minimization in (3) with weighted  $\ell_1$  minimization

$$\underset{z}{\text{minimize}} \quad \|z\|_{1,w} \quad \text{subject to} \quad \|Az - y\|_2 \leq \epsilon, \quad (4)$$

where  $w \in [0, 1]^N$  and  $\|z\|_{1,w} := \sum_i w_i |z_i|$  is the weighted  $\ell_1$  norm. In particular, in the methods that we describe here (including our own proposed method), the main idea is to choose  $w$  such that the entries of  $x$  that are “expected” to be large are penalized less in this weighted objective function.

The recovery of compressively sampled signals using prior support information has been previously studied in the literature; see, e.g., [6]–[10]. Early work by Borries et al. [6] demonstrated empirically that incorporating support information of a signal with a sparse discrete Fourier transform (DFT) allows for the number of compressed sensing measurements to be reduced by exactly the size of the known part of the support. Borries et al. achieve this by using a weighted  $\ell_1$  minimization approach with zero weights on the known support.

More recently, Vaswani and Lu [7]–[9] proposed a modified compressed sensing approach that again incorporates known support elements using a weighted  $\ell_1$  minimization approach with zero weights on the known support. Their work derives sufficient recovery conditions for the noise free case (i.e., set  $e = 0$  in (1) and  $\epsilon = 0$  in (4)) that are weaker than the analogous  $\ell_1$  minimization conditions of [2] in the case where a large proportion of the support is known. This work is supplemented by a regularized modified compressed sensing approach that deals with noisy measurements [9].

A similar method is proposed by Khajehnejad et al. [10] for the recovery of compressively sampled signals with support information. The performance of this method is analyzed using a Grassman angle approach. Prior information is defined in terms of two disjoint sets that partition  $\{1, \dots, N\}$ . The elements in the first set have a probability  $P_1$  of being nonzero, and the elements in the second set have a probability  $P_2$  of being nonzero, where  $P_1 \neq P_2$ . The authors propose weighted  $\ell_1$  minimization to recover the unknown vector where different weights  $w_1$  and  $w_2$  are assigned to the elements in the two sets. In particular, they find the class of signals  $x$ , depending on  $P_j$  and  $w_j$ ,  $j = 1, 2$ , which can be recovered with high probability using weighted  $\ell_1$ .

### C. Contributions

In this paper we adopt the weighted  $\ell_1$  minimization approach described by (4). Given a support estimate  $\tilde{T} \subset \{1, 2, \dots, N\}$  for  $x$ , we set  $w_j = \omega \in [0, 1]$  whenever  $j \in \tilde{T}$ , and  $w_j = 1$  otherwise. Unlike Borries et al. or Vaswani et al., in our results we allow  $\omega$  to be non-zero. We derive stability and robustness guarantees for weighted  $\ell_1$  minimization that generalize the results of [2]. Our results take into consideration the accuracy of the support estimate. In particular, we prove that if the (partial) support estimate is at least 50% accurate, then weighted  $\ell_1$  minimization outperforms standard  $\ell_1$  minimization in terms of accuracy, stability, and robustness. Finally, we note that when  $\omega = 0$ , our results hold under weaker conditions than those in [7].

In Section II, we review the  $\ell_1$  recovery guarantees of [2]. In Section III, we state our main result and compare our theoretical results with standard  $\ell_1$  recovery as well as the results of [7], [8]. In Sections IV and V, we present the outcome of numerical experiments on synthetic and on audio and video signals. We conclude with the proof of our main theorem in Section VI.

## II. COMPRESSED SENSING OVERVIEW

Consider an arbitrary signal  $x \in \mathbb{R}^N$  and let  $x_k \in \Sigma_k^N$  be its best  $k$ -term approximation. Let  $T_0 = \text{supp}(x_k)$ , where  $T_0 \subseteq \{1, \dots, N\}$  and  $|T_0| \leq k$ . We wish to reconstruct the signal  $x$  from  $y = Ax + e$ , where  $A$  is a known  $n \times N$  measurement matrix with  $n \ll N$ , and  $e$  denotes the (unknown) measurement error that satisfies  $\|e\|_2 \leq \epsilon$  for some known margin  $\epsilon > 0$ .

As we mentioned in the introduction, it was shown in [2] that  $x$  can be stably and robustly recovered from the measurements  $y$  by solving the optimization problem (2) if the measurement matrix  $A$  has the *restricted isometry property* (RIP), also defined by [2].

**Definition 1.** The restricted isometry constant  $\delta_k$  of a matrix  $A$  is the smallest number such that for all  $k$ -sparse vectors  $u \in \Sigma_k^N$ ,

$$(1 - \delta_k)\|u\|_2^2 \leq \|Au\|_2^2 \leq (1 + \delta_k)\|u\|_2^2. \quad (5)$$

Using the RIP, [2] provides conditions and bounds for stable and robust recovery of  $x$  by solving (3).

**Theorem 2** (Candès, Romberg, Tao [2]). *Suppose that  $x$  is an arbitrary vector in  $\mathbb{R}^N$ , and let  $x_k$  be the best  $k$ -term approximation of  $x$ . Suppose that there exists an  $a \in \frac{1}{k}\mathbb{Z}$  with  $a > 1$  and*

$$\delta_{ak} + a\delta_{(1+a)k} < a - 1. \quad (6)$$

Then the solution  $x^*$  to (3) obeys

$$\|x^* - x\|_2 \leq C_0 \epsilon + C_1 k^{-1/2} \|x - x_k\|_1. \quad (7)$$

*Remark 2.1.* The constants in Theorem 2 are explicitly given by

$$C_0 = \frac{2(1+a^{-1/2})}{\sqrt{1-\delta_{(a+1)k}-a^{-1/2}\sqrt{1+\delta_{ak}}}}, \quad C_1 = \frac{2a^{-1/2}(\sqrt{1-\delta_{(a+1)k}}+\sqrt{1+\delta_{ak}})}{\sqrt{1-\delta_{(a+1)k}-a^{-1/2}\sqrt{1+\delta_{ak}}}}. \quad (8)$$

From Theorem 2, one can see that if  $A$  satisfies (the slightly stronger condition)

$$\delta_{(a+1)k} < \frac{a-1}{a+1}, \quad (9)$$

then the constrained  $\ell_1$  minimization problem in (3) recovers  $x$  with an approximation error that scales well with measurement noise and the “compressibility” of  $x$ . Moreover, if  $x$  is sufficiently sparse (i.e.,  $x = x_k$ ), and the measurement process is noise-free, then Theorem 2 guarantees exact recovery of  $x$  from  $y$ .

### III. COMPRESSED SENSING WITH PARTIAL SUPPORT ESTIMATION

In this section, we present our main result showing that weighted  $\ell_1$  minimization can be used to stably and robustly recover sparse and compressible signals from noisy measurements when there is partial (and possibly partly inaccurate) prior support information. Our result holds under weaker sufficient conditions than its counterpart for  $\ell_1$  minimization when the support estimate is more than 50% accurate. Moreover, it results in smaller error bounds. We also compare our results with the modified compressed sensing approach proposed in [7].

#### A. Weighted $\ell_1$ minimization with estimated support

Let  $T_0$  be the support of  $x_k$ , and let  $\tilde{T}$ , the support estimate, be a subset of  $\{1, 2, \dots, N\}$  with cardinality  $k_1 := |\tilde{T}| = \rho k$ , where  $0 \leq \rho \leq a$  for some  $a > 1$ . As before, we wish to recover an arbitrary vector  $x \in \mathbb{R}^N$  from noisy compressive measurements  $y = Ax + e$ , where  $e$  satisfies  $\|e\|_2 \leq \epsilon$ . To recover  $x \in \mathbb{R}^N$ , we now consider the weighted  $\ell_1$  minimization problem with the following choice of weights:

$$\underset{z}{\text{minimize}} \quad \|z\|_{1,w} \quad \text{subject to} \quad \|Az - y\|_2 \leq \epsilon \quad \text{with} \quad w_i = \begin{cases} 1, & i \in \tilde{T}^c, \\ \omega, & i \in \tilde{T}. \end{cases} \quad (10)$$

Above  $0 \leq \omega \leq 1$  and  $\|z\|_{1,w}$  is as defined before in (4). Next, we present our main result.

**Theorem 3.** Let  $x$  be in  $\mathbb{R}^N$  and let  $x_k$  be its best  $k$ -term approximation, supported on  $T_0$ . Let  $\tilde{T} \subset \{1, \dots, N\}$  be an arbitrary set and define  $\rho$  and  $\alpha$  as before such that  $|\tilde{T}| = \rho k$  and  $|\tilde{T} \cap T_0| = \alpha \rho k$ . Suppose that there exists an  $a \in \frac{1}{k}\mathbb{Z}$ , with  $a \geq (1 - \alpha)\rho$ ,  $a > 1$ , and

$$\delta_{ak} + \frac{a}{(\omega + (1 - \omega)\sqrt{1 + \rho - 2\alpha\rho})^2} \delta_{(a+1)k} < \frac{a}{(\omega + (1 - \omega)\sqrt{1 + \rho - 2\alpha\rho})^2} - 1, \quad (11)$$

for some given  $0 \leq \omega \leq 1$ . Then the solution  $x^*$  to (10) obeys

$$\|x^* - x\|_2 \leq C'_0 \epsilon + C'_1 k^{-1/2} \left( \omega \|x - x_k\|_1 + (1 - \omega) \|x_{\tilde{T}^c \cap T_0^c}\|_1 \right). \quad (12)$$

The proof of the theorem is presented in section VI.

*Remark 3.1.* Note that the parameters in Theorem 3 specify two important ratios:  $\rho$  determines the ratio of the size of the estimated support to the size of the actual support of  $x_k$  (or the support of  $x$  if  $x$  is  $k$ -sparse). On the other hand,  $\alpha$  determines the ratio of the number of indices in  $\text{supp}(x_k)$  that were accurately estimated in  $\tilde{T}$  to the size of  $\tilde{T}$ . Specifically,  $\alpha = \frac{|\tilde{T} \cap T_0|}{|\tilde{T}|}$ .

*Remark 3.2.* The constants  $C'_0$  and  $C'_1$  are explicitly given by the expressions

$$C'_0 = \frac{2 \left( 1 + \frac{\omega + (1 - \omega)\sqrt{1 + \rho - 2\alpha\rho}}{\sqrt{a}} \right)}{\sqrt{1 - \delta_{(a+1)k}} - \frac{\omega + (1 - \omega)\sqrt{1 + \rho - 2\alpha\rho}}{\sqrt{a}} \sqrt{1 + \delta_{ak}}}, \quad C'_1 = \frac{2a^{-1/2} (\sqrt{1 - \delta_{(a+1)k}} + \sqrt{1 + \delta_{ak}})}{\sqrt{1 - \delta_{(a+1)k}} - \frac{\omega + (1 - \omega)\sqrt{1 + \rho - 2\alpha\rho}}{\sqrt{a}} \sqrt{1 + \delta_{ak}}}. \quad (13)$$

Consequently, Theorem 3, with  $\omega = 1$ , reduces to the stable and robust recovery theorem of [2], which we stated above—see Theorem 2.

*Remark 3.3.* It is sufficient that  $A$  satisfies

$$\delta_{(a+1)k} < \hat{\delta}^{(\omega)} := \frac{a - (\omega + (1 - \omega)\sqrt{1 + \rho - 2\alpha\rho})^2}{a + (\omega + (1 - \omega)\sqrt{1 + \rho - 2\alpha\rho})^2} \quad (14)$$

for Theorem 3 to hold, i.e., to guarantee stable and robust recovery of the signal  $x$  from measurements  $y = Ax + e$  (with constants  $C'_0$  and  $C'_1$  given in (13) and (14)).

*Remark 3.4.* Theorems 2 and 3 guarantee stable and robust recovery for matrices  $A$  satisfying a condition on  $\delta_{(a+1)k}$  with  $a > 1$ . A slightly different approach was used by Candès [11] to handle the case  $a = 1$ . Candès proved that if  $\delta_{2k} < (\sqrt{2} + 1)^{-1}$ , then  $\ell_1$  minimization (3) achieves stable and robust recovery. Following the same technique, with appropriate modifications to handle the weighted  $\ell_1$  objective, we

can derive the analogous alternative sufficient condition

$$\delta_{2k} < \left( \sqrt{2}(\omega + (1 - \omega)\sqrt{1 + \rho - 2\alpha\rho}) + 1 \right)^{-1}, \quad (15)$$

which guarantees stable and robust recovery using weighted  $\ell_1$  minimization (10). We omit the details of this calculation.

### B. Comparison to standard $\ell_1$ recovery

In this section, we compare the sufficient conditions for Theorem 3 and Theorem 2 as well as the associated constants of these two theorems. The following observation is easy to verify.

**Proposition 4.** *Let  $C_0, C_1, C'_0$ , and  $C'_1$  be as above. Then*

- (i) *If  $\omega = 1$ , then  $C'_0 = C_0$ ,  $C'_1 = C_1$ , and the sufficient conditions for Theorem 3, given in (11), are identical to those of Theorem 2, given in (6).*
- (ii) *If  $\alpha = 0.5$ , then, again  $C'_0 = C_0$ ,  $C'_1 = C_1$ , and the sufficient conditions for Theorem 3, given in (11), are identical to those of Theorem 2, given in (6).*
- (iii) *Suppose  $0 \leq \omega < 1$ . Then  $C'_0 < C_0$  and  $C'_1 < C_1$  if and only if  $\alpha > 0.5$ .*

Next, we illustrate how the slightly stronger sufficient conditions given in (14) and the respective stability constants vary with  $\alpha$  and  $\omega$ . Recall that when  $\omega = 1$ , (14) reduces to (9). In Figure 1 (a), we plot, for different values of  $\alpha$ ,  $\hat{\delta}^{(\omega)}$ , as defined in (14), versus  $\omega$ , where we set the parameter  $a = 3$ . We observe that as  $\alpha$  increases the sufficient condition on the RIP constant becomes weaker, allowing for a wider class of measurement matrices  $A$ . For example, with  $a = 3$ , when 70% of the support estimate is accurate, with  $\omega = 0.2$  it suffices to have  $\hat{\delta}^{(\omega)} < 0.763$ , compared with  $\hat{\delta}^{(1)} < 0.5$  for  $\ell_1$  minimization. figures 1 (b) and (c) illustrate that for a fixed matrix  $A$ , the constants  $C'_0$  and  $C'_1$  decrease as  $\alpha$  increases. Note that compared to setting  $\omega = 0$ , assigning non-zero weights  $\omega$  adds robustness to the weighted  $\ell_1$  problem in the case when  $\alpha < 0.5$ , i.e., when we have an inaccurate support estimate  $\tilde{T}$  with more than half the entries falling outside the support of the best  $k$ -term approximation of  $x$ . This could be beneficial in applications where the accuracy of the support estimates vary significantly from one signal to the next. Furthermore, in numerical experiments (see Section IV) we observe that using non-zero weights improves the quality of the reconstruction, especially in the noisy and compressible settings, not only when  $\alpha < 0.5$  but also in some cases where  $\alpha > 0.5$ . A mathematical understanding of this behavior and of how to optimally choose the weight  $\omega$  is beyond the scope of this paper.

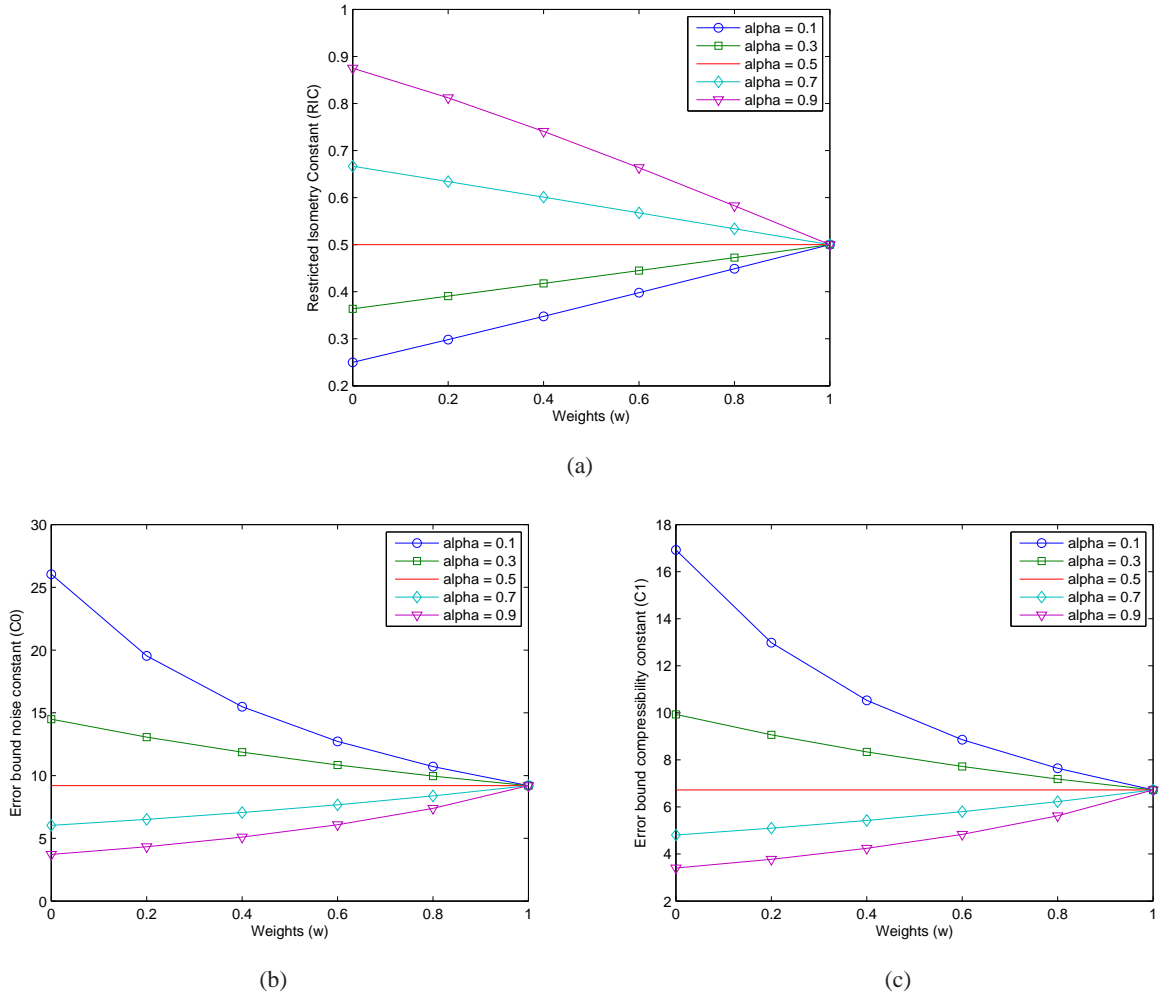


Fig. 1: Comparison of the sufficient conditions for recovery and stability constants for weighted  $\ell_1$  reconstruction with various of  $\alpha$ . In all the figures, we set  $a = 3$  and  $\rho = 1$ . (a)  $\hat{\delta}^{(\omega)}$  vs.  $\omega$ , (b)  $C'_0$  vs.  $\omega$ , (c)  $C'_1$  vs.  $\omega$ . In (b) and (c) we fix  $\delta_{(a+1)k} = 0.1$ .

### C. The zero weight case: $\omega = 0$

One special case of the weighted  $\ell_1$  problem that is of interest is the zero weight case, i.e., set  $\omega = 0$  in (10). It can be seen from Figure 1 that recovery using weighted  $\ell_1$  minimization (10) achieves the smallest error bound constants at  $\omega = 0$  when  $\alpha > 0.5$ . On the other hand, the recovery performance is worst when  $\omega = 0$  and  $\alpha < 0.5$ , i.e., when the support estimate is highly inaccurate.

Several contributions in the literature adopt the zero-weight approach, mainly in applications where prior support information is assumed to be highly accurate, i.e.,  $\alpha$  is close to 1, e.g., see [6], [7], [9]. The most recent study to address this problem is the work by Vaswani and Lu [7] where a sufficient



condition in terms of the RIP of the matrix  $A$  is derived for exact recovery in the noise free case. Another work by the same authors [9] addresses the noisy case, however, the recovery algorithm in this case is different from (10) in that the objective function is modified to include a regularization term. The sufficient condition derived in Corollary 1 of [7] is expressed as follows:

$$2\delta_{2u} + \delta_{3u} + \delta_k + \delta_{k+u}^2 + 2\delta_{k+2u}^2 < 1, \quad (16)$$

where  $u = (1 - \alpha\rho)k$  is the size of the unknown support. Recall that  $\alpha$  is such that  $\alpha\rho k$  is the size of the known support.

Below we compare our condition (15) with that of [7] given in (16) for different values of the unknown support size  $u$ . We consider the case  $\rho = 1$ ,  $u > 0$ , and  $n/N = 0.5$ . Thus, (15) reduces to

$$\delta_{2k} < \frac{1}{2\sqrt{u/k} + 1}. \quad (17)$$

Since the two sufficient conditions, i.e., (17) and (16), are expressed in terms of RIP constants of different-sized submatrices of  $A$ , a simple comparison of the upper bounds is not informative. For this reason, we restrict our attention to measurement matrices drawn from the Gaussian ensemble and we estimate the associated RIP constants (i.e.,  $\delta_{2k}, \delta_{2u}, \dots$ ) for such matrices using the bounds derived in [12]. In particular, we calculate the ratios  $u/k$  that satisfy the conditions (16) and (17), respectively, and plot the results in Figure 2. Observe that for the same measurement matrix  $A$  and sparsity level  $k/n$ , our sufficient condition guarantees the recovery of  $k$ -sparse signals with significantly less accurate prior support information compared to the condition of Vaswani et al. [7].

It is clear in Figure 2 that our recovery guarantees are superior to those of [7] at least when the aspect ratio of the measurement matrix is  $n/N = 0.5$ . Next, we shall focus on cases where we have a highly accurate estimate of the full support of the  $k$ -sparse vector  $x$ . In other words, we set  $\rho = 1$  as above and consider values of  $\alpha$  that are close to 1. For these cases, we will compare our theoretical guarantees to those of [7] for various values of the measurement matrix aspect ratio. To that end, we observe that the left-hand side of (16) is increasing in  $u$ . Thus, for any  $u$ , (16) can hold only if

$$\delta_k + 3\delta_k^2 < 1 \implies \delta_k < 0.4343,$$

which is obtained by setting  $u = 0$  in (16) and observing that  $\delta_0 = 0$  by definition. On the other hand, using the bounds from [12], we can estimate  $\delta_{2k}$  and find the corresponding range of  $u$  for (17) to hold in the case when  $A$  is a Gaussian random matrix. The upper bound on the range of  $u/k$  for various

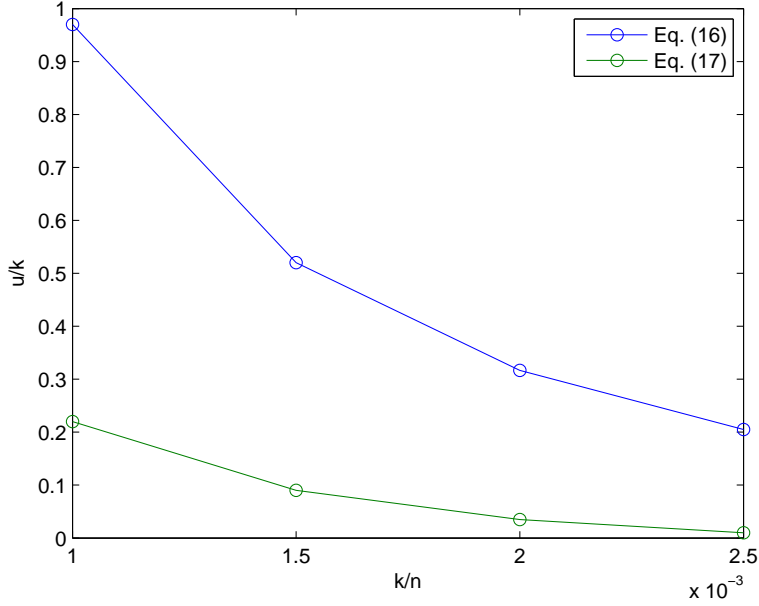


Fig. 2: Comparison between the values of  $u/k$  that satisfy each of the sufficient conditions (16) and (17). The measurement matrix has Gaussian entries with  $n/N = 0.5$ .

aspect ratios of the measurement matrix is reported in Table I. We conclude that in various cases with different measurement matrix aspect ratios our theoretical results guarantee recovery while the results of [7] fail to provide any recovery guarantee.

TABLE I: Maximum unknown support size  $u/k$  for which (17) holds while (16) fails to hold. Here for a given aspect ratio  $n/N$ , we compute the value of  $k/n$  for which  $\delta_k = 0.4343$ . This value, using (17), yields the corresponding bound on  $u/k$ .

$n/N$	$k/n$	$\delta_k$	$\delta_{2k}$	$u/k$
0.1	0.0029	0.4343	0.6153	0.0978
0.2	0.0031	0.4343	0.6139	0.0989
0.3	0.003218	0.4343	0.61176	0.1007
0.4	0.003315	0.4343	0.61077	0.1015
0.5	0.003394	0.4343	0.60989	0.1023

We finish this section by comparing the recovery guarantees we obtain in the zero-weight case with conditions that guarantee recovery via  $\ell_1$  minimization without using any prior support information. To this end, we present the phase diagrams of measurement matrices  $A$  with Gaussian entries that satisfy the conditions on the restricted isometry constants  $\delta_{(a+1)k}$  given in (9) and (14) with  $\omega = 0$ , respectively. We use the bounds derived in [12] and plot the curves in Figure 3 for matrices satisfying the sufficient

conditions on  $\delta_{4k}$  with  $\rho = 1$  and  $\alpha = 0.3, 0.6$ , and  $0.8$ .

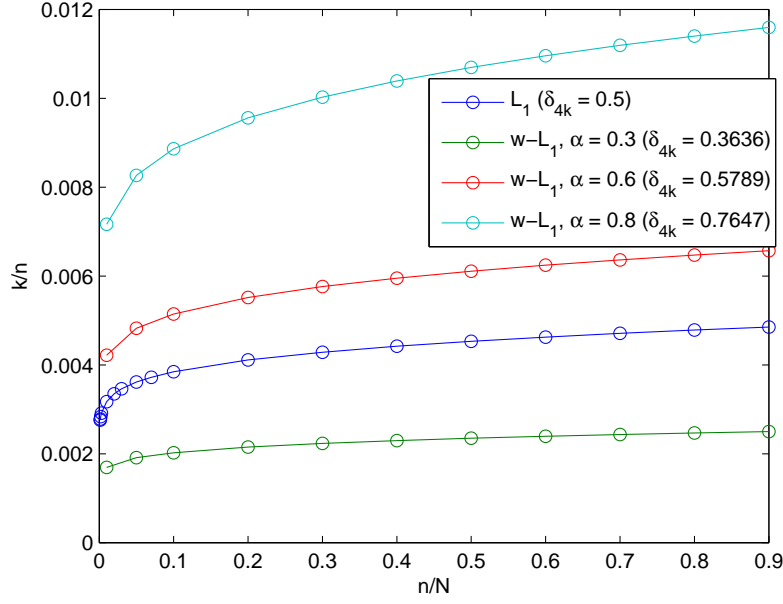


Fig. 3: Comparison between the phase diagrams of measurement matrices with Gaussian entries satisfying the sufficient recovery conditions of standard  $\ell_1$  minimization and weighted  $\ell_1$  minimization with  $\omega = 0$  and  $\alpha = 0.3, 0.6$ , and  $0.8$ . The plots are calculated using the upper bounds on the restricted isometry constants derived in [12].

#### IV. NUMERICAL EXAMPLES

In this section, we present numerical experiments that illustrate the benefits of using weighted  $\ell_1$  minimization to recover sparse and compressible signals when partial prior support information (which is possibly inaccurate) is available. To that end, we compare the recovery capabilities of standard  $\ell_1$  and weighted  $\ell_1$  minimization for a suite of synthetically generated sparse and compressible signals. In all of our experiments, we use SPGL1 [13], [14] to solve the standard and weighted  $\ell_1$  minimization problems.

##### A. The sparse case

We first generate signals  $x$  with an ambient dimension  $N = 500$  and fixed sparsity  $k = 40$ . We compute the (noisy) compressed measurements of  $x$  using a Gaussian random measurement matrix  $A$  with dimensions  $n \times N$  where we vary  $n$  between 80 and 200 with an increment of 20. In the experiments where the measurements are noisy, we set  $\epsilon = \|x\|/20$ .

Figure 4 shows the average reconstruction signal to noise ratio (SNR) over 20 experiments when using weighted  $\ell_1$  minimization depending on the number of measurements, both in the noise-free and noisy cases. The SNR is measured in dB and is given by

$$\text{SNR}(x, x^*) = 10 \log_{10} \left( \frac{\|x\|_2^2}{\|x - x^*\|_2^2} \right), \quad (18)$$

where  $x$  is the true signal and  $x^*$  is the recovered signal. The recovery is done via (10) using a support estimate of size  $|\tilde{T}| = 40$  (i.e.,  $\rho = 1$ ) where

- the accuracy  $\alpha$  of the support estimate ranges between zero and 1,
- the constant weight  $\omega$  ranges between zero and 1 (recall that when  $\omega = 1$  (10) is equivalent to standard  $\ell_1$  minimization).

Figure 4 (a) illustrates that in the noise free case, the experimental results are consistent with the theoretical bounds derived in Theorem 3. More specifically, it can be seen that when  $\alpha \geq 0.5$  the best recovery is achieved for a weight  $\omega = 0$  whereas a  $\omega = 1$  results in the worst SNR. On the other hand, when  $\alpha < 0.5$  the performance of the recovery algorithms is shifted towards larger values of  $\omega$  in the severely underdetermined cases (small  $n$ ).

*Remark 4.1.* Recall from Section III-B—see Figure 1—that when  $x$  is sparse and  $\alpha \geq 0.5$ ,  $\omega = 0$  results in the smallest error bound constants. Otherwise, i.e., when  $\alpha < 0.5$ ,  $\omega = 1$  minimizes the error constants. However, this does not match entirely with our experimental observations. It can be seen from Figure 4 (b) that, in general, the best recovery is obtained for intermediate values of  $\omega$ .

To explain this behaviour, consider the case where the measurement matrix does not satisfy the RIP conditions for the full recovery of a  $k$ -sparse  $x$  via weighted  $\ell_1$  minimization. In such cases,  $x$  can be regarded as compressible: Fix  $\hat{k} < k$  be such that Theorem 3 holds for all  $\hat{k}$ -sparse signals and for all  $\omega \in [0, 1]$ . Suppose  $\hat{T}$  is the support of the best  $\hat{k}$  term approximation of  $x$ . Then Theorem 3 guarantees stable and robust recovery of  $x$  where the recovery error is bounded by

$$\|x^* - x\|_2 \leq \frac{C'_1(\omega)}{\sqrt{\hat{k}}} (\omega \|x_{\hat{T}^c}\|_1 + (1 - \omega) \|x_{\tilde{T}^c \cap \hat{T}^c}\|_1),$$

where  $\tilde{T}$  is the prior support estimate. Denote by  $\hat{\alpha} = \frac{|\hat{T} \cap \tilde{T}|}{|\tilde{T}|}$  and note that since  $\hat{T} \subset T_0$ , then  $\hat{\alpha} < \alpha$ . Focusing our attention on the case when  $\hat{\alpha} < 0.5$  (where it is observed that  $0 < \omega < 1$  results in the best recovery), we make the following observations:

- The constant  $C'_1$  in the error bound above increases as  $\omega$  goes to zero (see Figure 1).
- Since  $\hat{T}^c \cap \tilde{T}^c \subseteq \hat{T}^c$ , the term  $\omega \|x_{\hat{T}^c}\|_1 + (1 - \omega) \|x_{\tilde{T}^c \cap \hat{T}^c}\|_1$  decreases as  $\omega$  goes to zero.

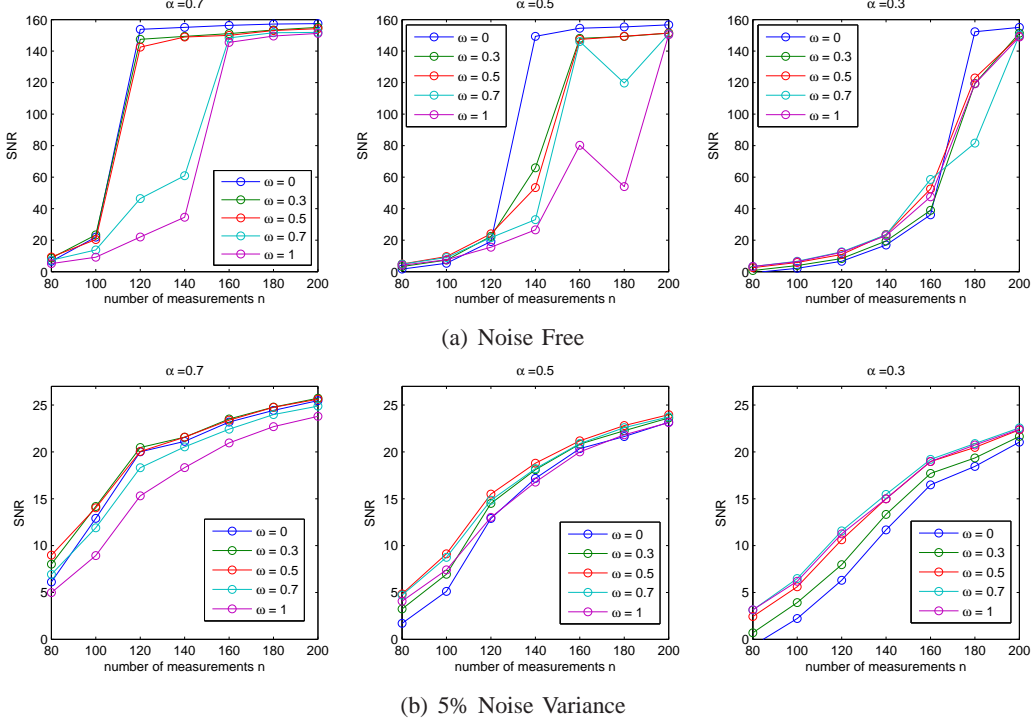


Fig. 4: Performance of weighted  $\ell_1$  recovery in terms of SNR averaged over 20 experiments for sparse signals  $x$  with  $k = 40$ ,  $N = 500$ , while varying the number of measurements  $n$ . From top left to right,  $\alpha = 0.7$ ,  $\alpha = 0.5$ , and  $\alpha = 0.3$ .

Therefore, for a fixed  $\hat{k}$ , there exists  $0 < \omega < 1$  that minimizes the product of the constant  $C'_1$  and the term  $\omega \|x_{\hat{T}^c}\|_1 + (1 - \omega) \|x_{\hat{T}^c \cap \hat{T}^c}\|_1$ . Consequently, when the algorithm cannot recover the full support of  $x$ , an intermediate value of  $\omega$  in  $(0, 1)$  may result in the smallest recovery error. A full mathematical analysis of the above observations needs to take into account all the interdependencies between  $\omega$ ,  $\hat{k}$ ,  $\hat{\alpha}$  as well as the parameters in Theorem 3 and is beyond the scope of this paper.

### B. The compressible case

Next, we generate a signal  $x$  whose coefficients decay like  $j^{-p}$  where  $j \in \{1, \dots, N\}$  and  $p > 1$ . In Figure 5, we illustrate the recovered signal SNR versus the size of the support estimate for  $p = 1.1$ . To calculate  $\alpha$  we set  $k = 40$ , i.e., we are interested in the best 40-term approximation. Notice that on average, a weight  $\omega \approx 0.5$  results in the best recovery. This behavior is consistent with the explanation provided above where an intermediate value of  $\omega$  balances the tradeoff between the error bound constants and the norm of the off-support components. We repeat this experiment with  $p = 1.5$ ,  $k = 20$  and  $p = 2$ ,  $k = 10$ . The results are reported in Figures 6 and 7, and show the same qualitative behaviour.

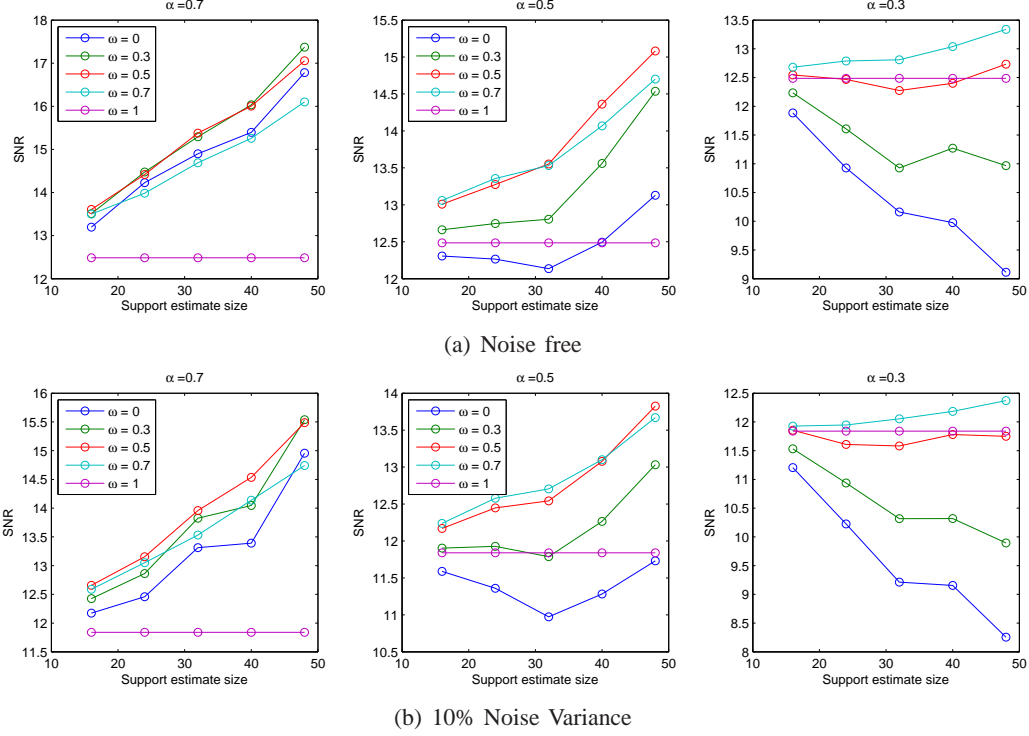


Fig. 5: Performance of weighted  $\ell_1$  recovery in terms of SNR averaged over 10 experiments for compressible signals  $x$  with  $n = 100$ ,  $N = 500$ . The coefficients decay with a power  $p = 1.1$ . The accuracy of the support estimate  $\alpha$  is calculated with respect to the best  $k = 40$  term approximation. From left to right,  $\alpha = 0.7$ ,  $\alpha = 0.5$ , and  $\alpha = 0.3$ .

## V. STYLIZED APPLICATIONS

In this section, we apply standard and weighted  $\ell_1$  minimization to recover real video and audio signals that are compressively sampled.

### A. Recovery of video signals

One natural application for weighted  $\ell_1$  minimization is video compressed sensing. Traditional video acquisition techniques capture a full frame (or image) in the pixel domain at a specific frame rate. The number of pixels acquired per image defines the spatial sampling rate, while the number of frames acquired per second defines the temporal sampling rate. Since the temporal sampling rate is usually high, a group of adjacent video frames are temporally correlated which is reflected in their spatial transform coefficients having nonzero entries in roughly the same locations.

Our aim here is to reduce the number of samples acquired for each video frame while keeping the same reconstruction quality by recovering using weighted  $\ell_1$  minimization. Here, we assume that for

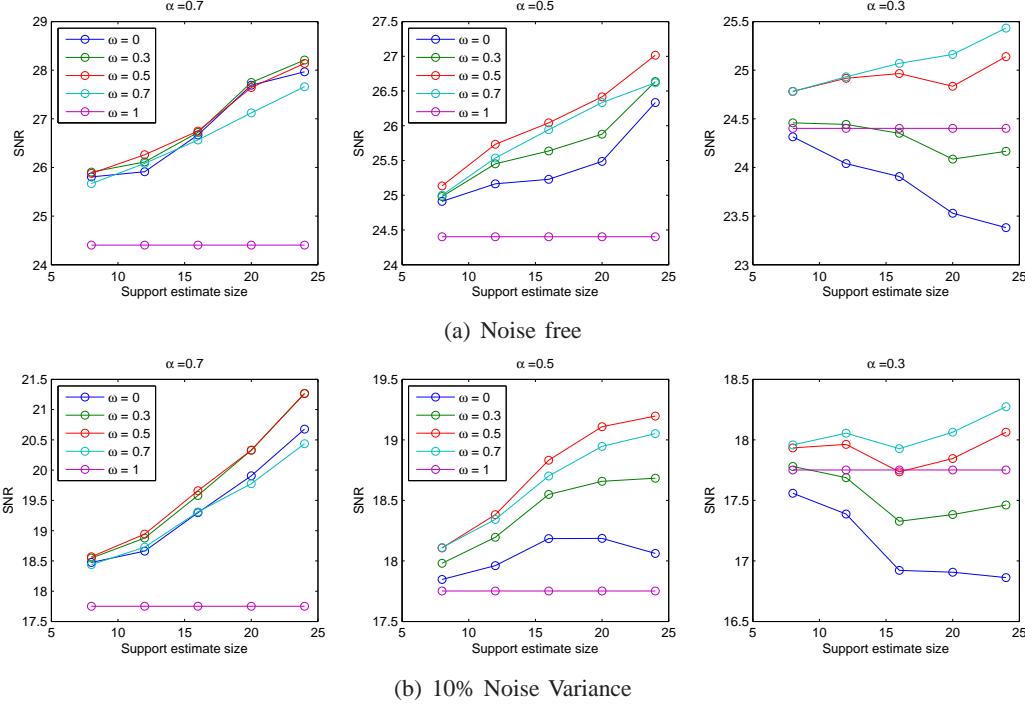


Fig. 6: Performance of weighted  $\ell_1$  recovery in terms of SNR averaged over 10 experiments for compressible signals  $x$  with  $n = 100$ ,  $N = 500$ . The coefficients decay with a power  $p = 1.5$ . The accuracy of the support estimate  $\alpha$  is calculated with respect to the best  $k = 20$  term approximation. From left to right,  $\alpha = 0.7$ ,  $\alpha = 0.5$ , and  $\alpha = 0.3$ .

every video frame  $j$ , the measurements  $y_j$ ,  $j \in \{0, 1, \dots, m-1\}$ , are acquired by storing the readings of a random subset of the CCD array with  $m$  denoting the total number of frames in the video sequence. Let  $n_j$  be the number of measurements acquired per frame  $j$  and  $N$  be the spatial resolution (number of pixels) to be recovered per frame. Let  $D$  be the spatial sparsifying transform. The measurement matrix  $A_j$  can then be written as  $A_j = R_j D$ , where  $R_j$  is an  $n_j \times N$  restriction matrix, and  $D$  is an orthonormal basis.

For the first frame,  $j = 0$ ,  $n_0$  measurements are captured and the transform coefficients  $x_0$  are recovered by solving the standard  $\ell_1$  minimization problem

$$\hat{x}_0 = \arg \min_x \|x\|_1 \text{ subject to } Ax = y_0.$$

For every subsequent frame  $j \geq 1$ , a support estimate  $\tilde{V}_j$  is chosen to be the union of the locations of the nonzero entries of  $\hat{x}_{j-1}$  and  $\hat{x}_{j-2}$  that contribute a certain percentage of the energy of  $\hat{x}_{j-1}$  and  $\hat{x}_{j-2}$ , respectively. Consequently, the coefficients  $\hat{x}_j$  are recovered from  $n_j < n_0$  measurements  $y_j$  by solving

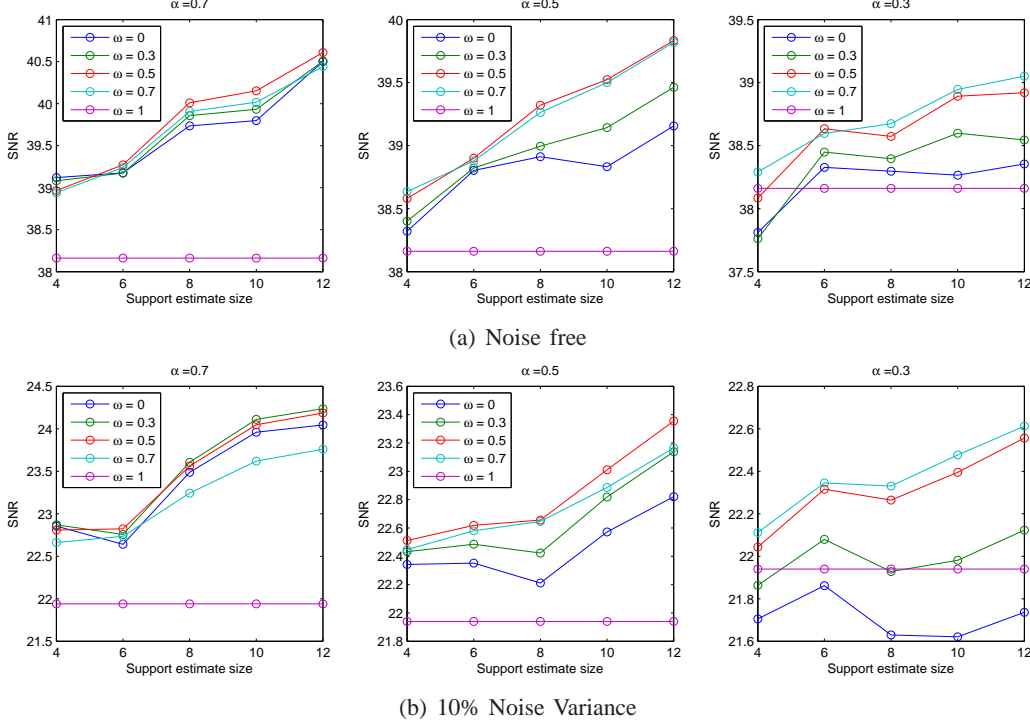


Fig. 7: Performance of weighted  $\ell_1$  recovery in terms of SNR averaged over 10 experiments for compressible signals  $x$  with  $n = 100$ ,  $N = 500$ . The coefficients decay with a power  $p = 2$ . The accuracy of the support estimate  $\alpha$  is calculated with respect to the best  $k = 10$  term approximation. From left to right,  $\alpha = 0.7$ ,  $\alpha = 0.5$ , and  $\alpha = 0.3$ .

the following weighted  $\ell_1$  minimization problem

$$\hat{x}_j = \arg \min_x \|x\|_{1,w} \text{ subject to } Ax = y_j, \quad \text{with } w_i = \begin{cases} 1, & i \in \tilde{V}_j^c, \\ \omega, & i \in \tilde{V}_j, \end{cases}$$

where  $0 \leq \omega \leq 1$ .

In our experiments, we use the Foreman sequence at QCIF resolution, i.e., every frame contains  $144 \times 176$  pixels. We only consider the luma (grayscale) component of the sequence. Every frame is split into four blocks, each of size  $N = 72 \times 88$  which are processed independently. We set  $n_0 = N/2$  and  $n_j = N/2.2$  and  $n_j = N/2.4$  for  $j \geq 1$ . The two dimensional discrete cosine transform (DCT) is used as the spatial sparsifying basis allowing for the support estimate  $\tilde{V}_j$  to include the DC component and the union of the AC coefficients that contribute to 97% of the energy in the AC coefficients of each of  $\hat{x}_{j-1}$  and  $\hat{x}_{j-2}$ . The signals  $\hat{x}_j$  are then recovered using weighted  $\ell_1$  minimization for  $\omega$  equal to 0, 0.1, 0.5, and 1.



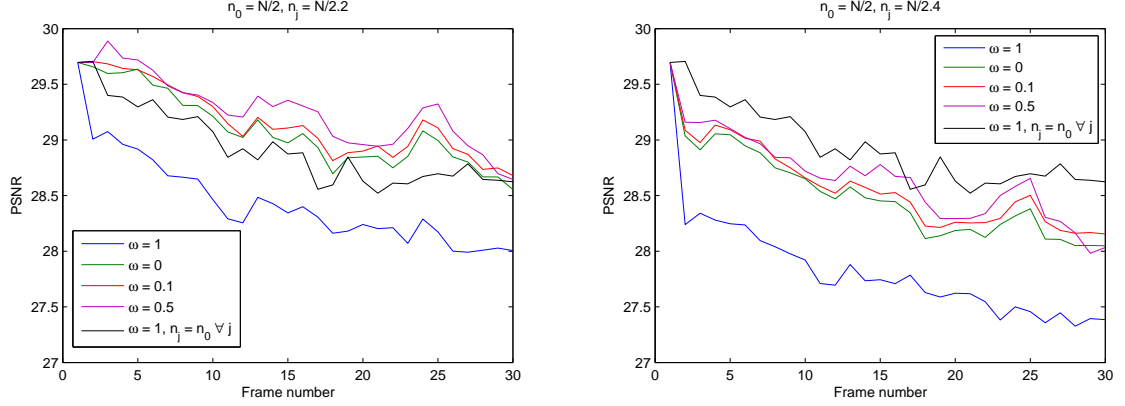


Fig. 8: Recovery of the first 30 frames of the Foreman sequence at QCIF resolution. The first frame is recovered from  $n_0 = N/2$  measurements, while the remaining frames are recovered from (a)  $n_j = N/2.2$  and (b)  $n_j = N/2.4$  measurements. Recovery is performed using weighted  $\ell_1$  minimization with  $\omega \in \{0, 0.1, 0.5, 1\}$ . The support estimate is derived from the union of the supports of the previous two frames. The black curve corresponds to the recovered PSNR using standard  $\ell_1$  minimization with a fixed number of measurements  $n_j = n_0, \forall j \in \{1, \dots, 30\}$ .

Figure 8 illustrates the recovery of the first 30 frames of the Foreman sequence using weighted  $\ell_1$  minimization. The reconstruction quality is reported in terms of the peak signal to noise ratio (PSNR) given by the expression

$$\text{PSNR}(x, \hat{x}) = 10 \log_{10} \left( \frac{N \times 255^2}{\|x - \hat{x}\|_2^2} \right). \quad (19)$$

The figure demonstrates that recovery with  $\omega = 0.5$  results in an improvement in PSNR averaging around 1 dB compared to standard  $\ell_1$  using the same number of measurements. A striking observation is that weighted  $\ell_1$  minimization outperforms standard  $\ell_1$  also with fewer measurements, i.e., in the case where  $n_j = n_0 \forall j$  for standard  $\ell_1$ , whereas  $n_j = n_0/2.2$  for weighted  $\ell_1$ .

### B. Recovery of audio signals

For our second stylized application, we examine the performance of weighted  $\ell_1$  minimization for the recovery of compressed sensing measurements of speech signals. In particular, the original signals are sampled at 44.1 kHz, but only 1/4th of the samples are retained (with their indices chosen randomly from the uniform distribution). This yields the measurements  $y = Rs$ , where  $s$  is the speech signal and  $R$  is a restriction (of the identity) operator. Consequently, by dividing the measurements into blocks of size  $N$ , we can write  $y = [y_1^T, y_2^T, \dots]^T$ . Here each  $y_j = R_j s_j$  is the measurement vector corresponding to the  $j$ th block of the signal, and  $R_j \in \mathbb{R}^{n_j \times N}$  is the associated restriction matrix. The signals we use

in our experiments consist of 21 such blocks. We make the following assumptions about speech signals:

- 1) The signal blocks are compressible in the DCT domain (for example, the MP3 compression standard uses a version of the DCT to compress audio signals.)
- 2) The support set corresponding to the largest coefficients in adjacent blocks does not change much from block to block.
- 3) Speech signals have large low-frequency coefficients.

Thus, for the reconstruction of the  $j$ th block, we choose the support estimate  $\tilde{T} = \tilde{T}^1 \cup \tilde{T}^2$ . Here,  $\tilde{T}^1$  is the set corresponding to frequencies up to 4kHz and  $\tilde{T}^2$  is the set corresponding to the largest  $n_j/16$  recovered coefficients of the previous block (for the first block  $\tilde{T}^2$  is empty). The results of experiments on two speech signals (one male and one female) with  $N = 2048$ , and  $\omega \in \{0, 1/6, 2/6, \dots, 1\}$  are illustrated in Figure 9.

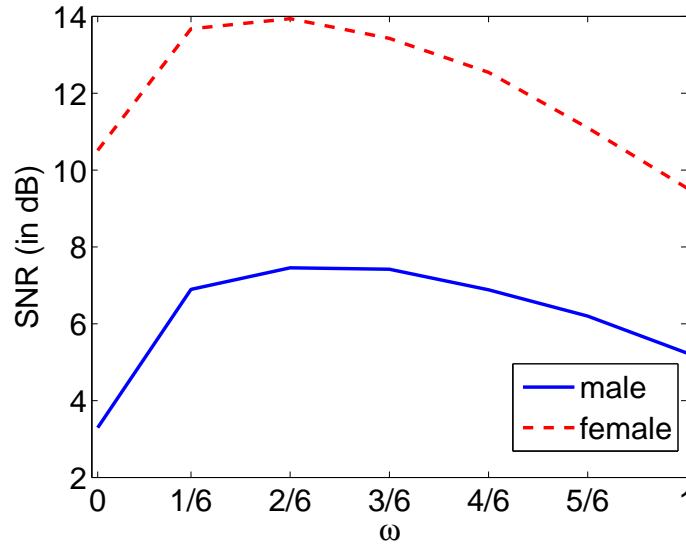


Fig. 9: SNRs of two reconstructed signals from compressed sensing measurements plotted against  $\omega$ . For both speech signals, an intermediate value of  $\omega$  yields the best performance.

## VI. PROOF OF THEOREM 3

Recall that  $\tilde{T}$ , an arbitrary subset of  $\{1, 2, \dots, N\}$ , is of size  $\rho k$  where  $0 \leq \rho \leq a$  and  $a$  is some number larger than 1. Let the set  $\tilde{T}_\alpha = T_0 \cap \tilde{T}$  and  $\tilde{T}_\beta = T_0^c \cap \tilde{T}$ , where  $|\tilde{T}_\alpha| = \alpha|\tilde{T}| = \alpha\rho k$  and  $\alpha + \beta = 1$ . Figure 10 illustrates these sets and shows the relationship to the weight vector  $w$ .

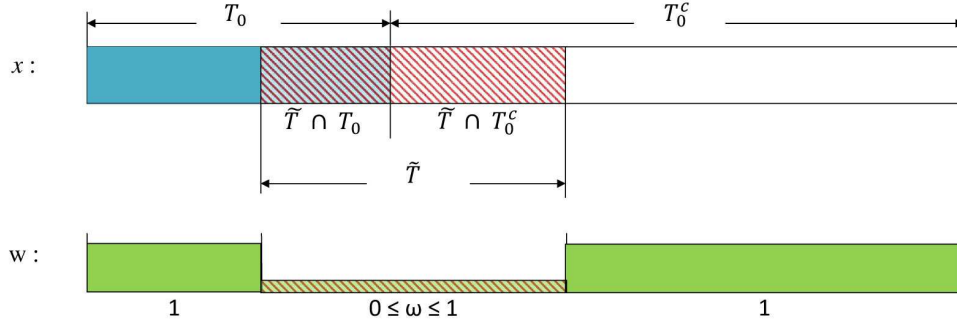


Fig. 10: Illustration of the signal  $x$  and weight vector  $w$  emphasizing the relationship between the sets  $T_0$  and  $\tilde{T}$ .

Let  $x^* = x + h$  be a minimizer of the weighted  $\ell_1$  problem (10). Then

$$\|x + h\|_{1,w} \leq \|x\|_{1,w}.$$

Moreover, by the choice of weights in (10), we have

$$\omega \|x_{\tilde{T}} + h_{\tilde{T}}\|_1 + \|x_{\tilde{T}^c} + h_{\tilde{T}^c}\|_1 \leq \omega \|x_{\tilde{T}}\|_1 + \|x_{\tilde{T}^c}\|_1.$$

Consequently,

$$\begin{aligned} & \|x_{\tilde{T}^c \cap T_0} + h_{\tilde{T}^c \cap T_0}\|_1 + \|x_{\tilde{T}^c \cap T_0^c} + h_{\tilde{T}^c \cap T_0^c}\|_1 + \omega \|x_{\tilde{T} \cap T_0} + h_{\tilde{T} \cap T_0}\|_1 + \omega \|x_{\tilde{T} \cap T_0^c} + h_{\tilde{T} \cap T_0^c}\|_1 \\ & \leq \|x_{\tilde{T}^c \cap T_0}\|_1 + \|x_{\tilde{T}^c \cap T_0^c}\|_1 + \omega \|x_{\tilde{T} \cap T_0}\|_1 + \omega \|x_{\tilde{T} \cap T_0^c}\|_1. \end{aligned}$$

Next, we use the forward and reverse triangle inequalities to get

$$\omega \|h_{\tilde{T} \cap T_0^c}\|_1 + \|h_{\tilde{T}^c \cap T_0^c}\|_1 \leq \|h_{\tilde{T}^c \cap T_0}\|_1 + \omega \|h_{\tilde{T} \cap T_0}\|_1 + 2 \left( \|x_{\tilde{T}^c \cap T_0^c}\|_1 + \omega \|x_{\tilde{T} \cap T_0^c}\|_1 \right).$$

Adding and subtracting  $\omega \|h_{\tilde{T}^c \cap T_0^c}\|_1$  on the left hand side, and  $\omega \|h_{\tilde{T}^c \cap T_0}\|_1$  on the right, we obtain

$$\begin{aligned} & \omega \|h_{\tilde{T} \cap T_0^c}\|_1 + \omega \|h_{\tilde{T}^c \cap T_0^c}\|_1 + \|h_{\tilde{T}^c \cap T_0^c}\|_1 - \omega \|h_{\tilde{T}^c \cap T_0^c}\|_1 \\ & \leq \omega \|h_{\tilde{T} \cap T_0}\|_1 + \omega \|h_{\tilde{T}^c \cap T_0}\|_1 + \|h_{\tilde{T}^c \cap T_0}\|_1 - \omega \|h_{\tilde{T}^c \cap T_0}\|_1 \\ & \quad + 2 \left( \omega \|x_{\tilde{T} \cap T_0^c}\|_1 + \omega \|x_{\tilde{T}^c \cap T_0^c}\|_1 + \|x_{\tilde{T}^c \cap T_0^c}\|_1 - \omega \|x_{\tilde{T}^c \cap T_0^c}\|_1 \right). \end{aligned}$$

Since  $\|h_{T_0^c}\|_1 = \|h_{\tilde{T} \cap T_0^c}\|_1 + \|h_{\tilde{T}^c \cap T_0^c}\|_1$ , this easily reduces to

$$\omega \|h_{T_0^c}\|_1 + (1-\omega) \|h_{\tilde{T}^c \cap T_0^c}\|_1 \leq \omega \|h_{T_0}\|_1 + (1-\omega) \|h_{\tilde{T}^c \cap T_0}\|_1 + 2 \left( \omega \|x_{T_0^c}\|_1 + (1-\omega) \|x_{\tilde{T}^c \cap T_0^c}\|_1 \right). \quad (20)$$

But, we can also write

$$\|h_{T_0^c}\|_1 = \omega\|h_{T_0}\|_1 + (1 - \omega)\|h_{\tilde{T}^c \cap T_0^c}\|_1 + (1 - \omega)\|h_{\tilde{T} \cap T_0^c}\|_1.$$

Combining the above with (20), we obtain

$$\begin{aligned} \Rightarrow \|h_{T_0^c}\|_1 &\leq \omega\|h_{T_0}\|_1 + (1 - \omega)\|h_{\tilde{T}^c \cap T_0^c}\|_1 + (1 - \omega)\|h_{\tilde{T} \cap T_0^c}\|_1 + 2\left(\omega\|x_{T_0^c}\|_1 + (1 - \omega)\|x_{\tilde{T}^c \cap T_0^c}\|_1\right) \\ &= \omega\|h_{T_0}\|_1 + (1 - \omega)\left(\|h_{\tilde{T}^c \cap T_0^c}\|_1 + \|h_{\tilde{T} \cap T_0^c}\|_1\right) + 2\left(\omega\|x_{T_0^c}\|_1 + (1 - \omega)\|x_{\tilde{T}^c \cap T_0^c}\|_1\right). \end{aligned}$$

Since, the set  $\tilde{T}_\alpha = T_0 \cap \tilde{T}$ , we can write  $\|h_{\tilde{T}^c \cap T_0^c}\|_1 + \|h_{\tilde{T} \cap T_0^c}\|_1 = \|h_{T_0 \cup \tilde{T} \setminus \tilde{T}_\alpha}\|_1$  and simplify the bound on  $\|h_{T_0^c}\|_1$  to the following expression:

$$\|h_{T_0^c}\|_1 \leq \omega\|h_{T_0}\|_1 + (1 - \omega)\|h_{T_0 \cup \tilde{T} \setminus \tilde{T}_\alpha}\|_1 + 2\left(\omega\|x_{T_0^c}\|_1 + (1 - \omega)\|x_{\tilde{T}^c \cap T_0^c}\|_1\right). \quad (21)$$

Next we sort the coefficients of  $h_{T_0^c}$  partitioning  $T_0^c$  it into disjoint sets  $T_j, j \in \{1, 2, \dots\}$  each of size  $ak$ , where  $a > 1$ . That is,  $T_1$  indexes the largest  $ak$  coefficients of  $h_{T_0^c}$ ,  $T_2$  indexes the second largest  $ak$  coefficients of  $h_{T_0^c}$ , and so on. Note that this gives  $h_{T_0^c} = \sum_{j \geq 1} h_{T_j}$ , with

$$\|h_{T_j}\|_2 \leq \sqrt{ak}\|h_{T_j}\|_\infty \leq (ak)^{-1/2}\|h_{T_{j-1}}\|_1. \quad (22)$$

Let  $T_{01} = T_0 \cup T_1$ , then using (22) and the triangle inequality we have

$$\begin{aligned} \|h_{T_{01}^c}\|_2 &\leq \sum_{j \geq 2} \|h_{T_j}\|_2 \leq (ak)^{-1/2} \sum_{j \geq 1} \|h_{T_j}\|_1 \\ &\leq (ak)^{-1/2} \|h_{T_0^c}\|_1. \end{aligned} \quad (23)$$

Combining the above expression with (21) we get

$$\|h_{T_{01}^c}\|_2 \leq (ak)^{-1/2} \left( \omega\|h_{T_0}\|_1 + (1 - \omega)\|h_{T_0 \cup \tilde{T} \setminus \tilde{T}_\alpha}\|_1 + 2\left(\omega\|x_{T_0^c}\|_1 + (1 - \omega)\|x_{\tilde{T}^c \cap T_0^c}\|_1\right) \right). \quad (24)$$

Next, consider the feasibility of  $x^*$  and  $x$ . Both vectors are feasible, so we have  $\|Ah\|_2 \leq 2\epsilon$  and

$$\begin{aligned} \|Ah_{T_{01}}\|_2 &\leq 2\epsilon + \|Ah_{T_{01}^c}\|_2 \leq 2\epsilon + \sum_{j \geq 2} \|Ah_{T_j}\|_2 \\ &\leq 2\epsilon + \sqrt{1 + \delta_{ak}} \sum_{j \geq 2} \|h_{T_j}\|_2. \end{aligned}$$

From (23) and (24) we get

$$\begin{aligned} \|Ah_{T_{01}}\|_2 &\leq 2\epsilon + 2\frac{\sqrt{1 + \delta_{ak}}}{\sqrt{ak}} \left( \omega\|x_{T_0^c}\|_1 + (1 - \omega)\|x_{\tilde{T}^c \cap T_0^c}\|_1 \right) \\ &\quad + \omega\frac{\sqrt{1 + \delta_{ak}}}{\sqrt{ak}}\|h_{T_0}\|_1 + (1 - \omega)\frac{\sqrt{1 + \delta_{ak}}}{\sqrt{ak}}\|h_{T_0 \cup \tilde{T} \setminus \tilde{T}_\alpha}\|_1 \end{aligned}$$

Noting that  $|T_0 \cup \tilde{T} \setminus \tilde{T}_\alpha| = (1 + \rho - 2\alpha\rho)k$ ,

$$\begin{aligned} \sqrt{1 - \delta_{(a+1)k}} \|h_{T_{01}}\|_2 &\leq 2\epsilon + 2\frac{\sqrt{1+\delta_{ak}}}{\sqrt{ak}} \left( \omega \|x_{T_0^c}\|_1 + (1 - \omega) \|x_{\tilde{T}^c \cap T_0^c}\|_1 \right) \\ &\quad + \omega \frac{\sqrt{1+\delta_{ak}}}{\sqrt{a}} \|h_{T_0}\|_2 + (1 - \omega) \frac{\sqrt{1+\delta_{ak}}}{\sqrt{a}} \sqrt{1 + \rho - 2\alpha\rho} \|h_{T_0 \cup \tilde{T} \setminus \tilde{T}_\alpha}\|_2. \end{aligned}$$

Since the set  $T_1$  contains the largest  $ak$  coefficients of  $h_{T_0^c}$  with  $a > 1$ , and  $|\tilde{T} \setminus \tilde{T}_\alpha| = (1 - \alpha)\rho k \leq ak$ , then  $\|h_{T_0 \cup \tilde{T} \setminus \tilde{T}_\alpha}\|_2 \leq \|h_{T_{01}}\|_2$ . We also have  $\|h_{T_0}\|_2 \leq \|h_{T_{01}}\|_2$ , thus

$$\|h_{T_{01}}\|_2 \leq \frac{2\epsilon + 2\frac{\sqrt{1+\delta_{ak}}}{\sqrt{ak}} \left( \omega \|x_{T_0^c}\|_1 + (1 - \omega) \|x_{\tilde{T}^c \cap T_0^c}\|_1 \right)}{\sqrt{1 - \delta_{(a+1)k}} - \frac{\omega + (1 - \omega)\sqrt{1 + \rho - 2\alpha\rho}}{\sqrt{a}} \sqrt{1 + \delta_{ak}}}. \quad (25)$$

Finally, using  $\|h\|_2 \leq \|h_{T_{01}}\|_2 + \|h_{T_{01}^c}\|_2$ , we combine (24) and (25) to get

$$\|h\|_2 \leq \frac{2 \left( 1 + \frac{\omega + (1 - \omega)\sqrt{1 + \rho - 2\alpha\rho}}{\sqrt{a}} \right) \epsilon + 2\frac{\sqrt{1 - \delta_{(a+1)k}} + \sqrt{1 + \delta_{ak}}}{\sqrt{ak}} \left( \omega \|x_{T_0^c}\|_1 + (1 - \omega) \|x_{\tilde{T}^c \cap T_0^c}\|_1 \right)}{\sqrt{1 - \delta_{(a+1)k}} - \frac{\omega + (1 - \omega)\sqrt{1 + \rho - 2\alpha\rho}}{\sqrt{a}} \sqrt{1 + \delta_{ak}}}, \quad (26)$$

with the condition that the denominator is positive, equivalently

$$\delta_{ak} + \frac{a}{(\omega + (1 - \omega)\sqrt{1 + \rho - 2\alpha\rho})^2} \delta_{(a+1)k} < \frac{a}{(\omega + (1 - \omega)\sqrt{1 + \rho - 2\alpha\rho})^2} - 1. \quad (27)$$

□

## REFERENCES

- [1] D. Donoho, “Compressed sensing,” *IEEE Transactions on Information Theory*, vol. 52, no. 4, pp. 1289–1306, 2006.
- [2] E. J. Candès, J. Romberg, and T. Tao, “Stable signal recovery from incomplete and inaccurate measurements,” *Communications on Pure and Applied Mathematics*, vol. 59, pp. 1207–1223, 2006.
- [3] —, “Robust uncertainty principles: exact signal reconstruction from highly incomplete frequency information,” *IEEE Transactions on Information Theory*, vol. 52, pp. 489–509, 2006.
- [4] D. Donoho and M. Elad, “Optimally sparse representation in general (nonorthogonal) dictionaries via  $\ell^1$  minimization,” *Proceedings of the National Academy of Sciences of the United States of America*, vol. 100, no. 5, pp. 2197–2202, 2003.
- [5] R. Robucci, J. Gray, L. K. Chiu, J. Romberg, and P. Hasler, “Compressive sensing on a cmos separable-transform image sensor,” *Proceedings of the IEEE*, vol. 98, no. 6, pp. 1089–1101, Jun. 2010.
- [6] R. von Borries, C. Miosso, and C. Potes, “Compressed sensing using prior information,” in *2nd IEEE International Workshop on Computational Advances in Multi-Sensor Adaptive Processing, CAMPSAP 2007.*, 12-14 2007, pp. 121 – 124.
- [7] N. Vaswani and W. Lu, “Modified-cs: Modifying compressive sensing for problems with partially known support,” *arXiv:0903.5066v4*, 2009.
- [8] —, “Modified-cs: Modifying compressive sensing for problems with partially known support,” in *IEEE International Symposium on Information Theory, ISIT 2009. I*, june 2009, pp. 488 – 492.

- [9] W. Lu and N. Vaswani, “Modified basis pursuit denoising(modified-bpdn) for noisy compressive sensing with partially known support,” in *IEEE International Conference on Acoustics Speech and Signal Processing (ICASSP)*, 2010, 14-19 2010, pp. 3926 – 3929.
- [10] M. Amin Khajehnejad, W. Xu, A. Salman Avestimehr, and B. Hassibi, “Weighted  $l_1$  minimization for sparse recovery with prior information,” in *IEEE International Symposium on Information Theory, ISIT 2009*, june 2009, pp. 483 – 487.
- [11] E. J. Candès, “The restricted isometry property and its implications for compressed sensing,” *Comptes rendus-Mathématique*, vol. 346, no. 9-10, pp. 589–592, 2008.
- [12] B. Bah and J. Tanner, “Improved bounds on restricted isometry constants for gaussian matrices,” *CoRR*, 2010. [Online]. Available: arXiv:1003.3299v2
- [13] E. van den Berg and M. P. Friedlander, “Probing the pareto frontier for basis pursuit solutions,” *SIAM Journal on Scientific Computing*, vol. 31, no. 2, pp. 890–912, 2008. [Online]. Available: <http://link.aip.org/link/?SCE/31/890>
- [14] —, “SPGL1: A solver for large-scale sparse reconstruction,” June 2007, <http://www.cs.ubc.ca/labs/scl/spgl1>.